Z. Phys. C – Particles and Fields 46, 15–23 (1990)

Zeitschrift für Physik C Particles and Fields

Inclusive π^0 and η meson production in electron positron interactions at $\sqrt{s} = 10$ GeV

ARGUS Collaboration

H. Albrecht, R. Gläser, G. Harder, A. Krüger, A. Nippe, T. Oest, M. Reidenbach, M. Schäfer, W. Schmidt-Parzefall, H. Schröder, H.D. Schulz, F. Sefkow, R. Wurth
DESY, Hamburg, Federal Republic of Germany

R.D. Appuhn, A. Drescher, C. Hast, G. Herrera, D. Kamp[1], H. Kolanoski, A. Lange, A. Lindner, R. Mankel, U. Matthiesen[2], H. Scheck, G. Schweda, B. Spaan, A. Walther, D. Wegener
Institut für Physik[3], Universität, Dortmund, Federal Republic of Germany

M. Paulini, K. Reim, U. Volland, H. Wegener
Physikalisches Institut[4], Universität Erlangen-Nürnberg, Federal Republic of Germany

W. Funk, J. Stiewe, S. Werner
Institut für Hochenergiephysik[5], Universität, Heidelberg, Federal Republic of Germany

J.C. Gabriel, A. Hölscher, W. Hofmann, S. Khan, J. Spengler
Max-Planck-Institut für Kernphysik, Heidelberg, Federal Republic of Germany

C.E.K. Charlesworth[6], K.W. Edwards[7], W.R. Frisken[8], H. Kapitza[7], R. Kutschke[6], D.B. MacFarlane[9], K.W. McLean[9], R.S. Orr[6], J.A. Parsons[6], P.M. Patel[9], J.D. Prentice[6], S.C. Seidel[6], J.D. Swain[6], G. Tsipolitis[9], T.-S. Yoon[6]
Institute of Particle Physics[10], Canada

S. Ball, R. Davis, N. Kwak
University of Kansas[11], Lawrence, KS, USA

T. Ruf, S. Schael, K.R. Schubert, K. Strahl, R. Waldi, S. Weseler
Institut für Experimentelle Kernphysik[12], Universität, Karlsruhe, Federal Republic of Germany

B. Boštjančič, G. Kernel, P. Križan, E. Križnič, M. Pleško
Institut J. Stefan and Oddelek za fiziko[13], Univerza v Ljubljani, Ljubljana, Yugoslavia

H.I. Cronström, L. Jönsson, A.W. Nilsson
Institute of Physics[14], University, Lund, Sweden

A. Babaev, M. Danilov, B. Fominykh, A. Golutvin, I. Gorelov, V. Lubimov, A. Rostovtsev, A. Semenov, S. Semenov, V. Shevchenko, V. Soloshenko, V. Tchistilin, I. Tichomirov, Yu. Zaitsev
Institute of Theoretical and Experimental Physics, Moscow, USSR

R. Childers, C.W. Darden
University of South Carolina[15], Columbia, SC, USA

Received 16 June 1989

[1] Now at Beiersdorf AG, Hamburg, FRG
[2] Now at St. Galler Stadtwerke, St. Gallen, Switzerland
[3] Supported by the German Bundesministerium für Forschung und Technologie, under contract number 054DO51P
[4] Supported by the German Bundesministerium für Forschung und Technologie, under contract number 054ER11P(5)
[5] Supported by the German Bundesministerium für Forschung und Technologie, under contract number 054HD24P
[6] University of Toronto, Toronto, Ontario, Canada
[7] Carleton University, Ottawa, Ontario, Canada
[8] York University, Downsview, Ontario, Canada
[9] McGill University, Montreal, Quebec, Canada
[10] Supported by the Natural Sciences and Engineering Research Council, Canada
[11] Supported by the U.S. National Science Foundation
[12] Supported by the German Bundesministerium für Forschung und Technologie, under contract number 054KA17P
[13] Supported by Raziskovalna skupnost Slovenije and the Internationales Büro KfA, Jülich
[14] Supported by the Swedish Research Council
[15] Supported by the U.S. Department of Energy, under contract DE-AS09-80ER10690

Abstract. We report on a high statistics study of π^0 and η production in continuum events and in direct decays of the $\Upsilon(1S)$ and $\Upsilon(2S)$ resonances. The measured production rates per event are $\langle n_{\pi^0}\rangle = 3.22 \pm 0.07 \pm 0.31$ $(3.97 \pm 0.23 \pm 0.38)$ and $\langle n_\eta\rangle = 0.19 \pm 0.04 \pm 0.04$ $(0.40 \pm 0.14 \pm 0.09)$ for continuum events (direct $\Upsilon(1S)$ decays).

1 Introduction

Most studies of hadron production in the Υ energy region have concentrated on the production of charged hadrons [1–4], with special emphasis on baryons [1, 2, 5, 6]. In this paper, the first high statistics study of π^0 and η meson production in this energy region is presented. The measurements allow a comparison of the fragmentation properties of $q\bar{q}$- and three gluon systems, with the aim of studying possible differences in the fragmentation of quarks and gluons. The study of the η sample is of particular interest in this context, since theoretical arguments exist for enhanced η production in gluon jets [7]. Moreover, experimental indications for such a difference have already been published [8]. The continuum data for π^0 meson production can be compared with the high statistics results collected at PETRA [9] and PEP [10] energies.

2 Data analysis

2.1 Data sample and event selection

The analysis is based on a data set collected with the ARGUS detector at the DORIS II storage ring at DESY. The data sample comprises an integrated luminosity of 36.5 pb^{-1} at various continuum energies around 10 GeV, 42.3 pb^{-1} on the $\Upsilon(1S)$, and 33.1 pb^{-1} on the $\Upsilon(2S)$ resonance. Details of the detector, the trigger and the event reconstruction techniques are discussed in [11].

Since the detector is triggered not only by multihadron events due to e^+e^- annihilation into $q\bar{q}$-pairs and direct decays of the Υ resonances but also by background from QED processes, beam-gas and beam-wall interactions and two-photon processes, global selection criteria are needed to suppress this background. By application of the event selection cuts described in [4] it is reduced to a negligible level of less than 3% which was accounted for in the systematic error. Background from radiative QED events is largely eliminated by requiring at least two photons to be detected in the calorimeter. Details on the event selection can be found in [12].

2.2 Reconstruction of photons

The following algorithm has been applied to reconstruct photons from the shower counter information. The recorded signal of each shower counter module is converted into an energy using a calibration constant determined for every module from Bhabha scattering events [13]. Neighbouring modules with signals are grouped into clusters. Trajectories of all reconstructed charged particles are then extrapolated to the shower counters. If at least one of the counters belonging to a cluster is hit by the extrapolated track the whole cluster is associated with this track. No attempt is made to disentangle overlapping clusters produced by a charged particle and a neutral. Depending on the topology of the multihadron event 10 to 15% of all photons are lost by such overlaps [12]. The remaining clusters are assumed to be photons.

For each photon candidate the center of gravity, S_{cog}, of the shower is calculated

$$S_{\text{cog}} = \frac{\sum_{i=1}^{n} s_i E_i}{\sum_{i=1}^{n} E_i}$$

where s_i is an appropriate coordinate and E_i the deposited energy in the i^{th} module. In the barrel region (z, φ) are chosen as coordinates, while in the end cap region (r, φ) are used. The centers of gravity S_{cog} are converted into the coordinates of the impact point S_{imp} using the results of a Monte Carlo simulation. The coordinates of the impact point can then be used to correct for inhomogeneities of the ARGUS electromagnetic calorimeter due to the support structure and the wave length shifter [13]. The impact point and the energy of the detected photon are determined by an iterative process which converges after a few steps.

Finally a special correction has to be applied for low energy photons ($E_\gamma \leqq 500$ MeV), because ADC signals are only recorded above a given threshold in order to suppress noise pulses. This cut is important for those counters which are hit by the tail of an electromagnetic shower. If a large amount of energy is deposited, e.g. by a Bhabha electron, this effect can be neglected, but for the low energy photons produced in π^0 meson decays, energy corrections up to 20% are necessary. We have derived the correction function directly from the data by calculating the mass of those π^0 mesons where one decay photon (γ_s) is detected in the shower counters while the other (γ_c) is converting in the beamtube and the e^+e^- pair is reconstructed in the drift chamber. In Fig. 1 the average reconstructed π^0 mass is shown as a function

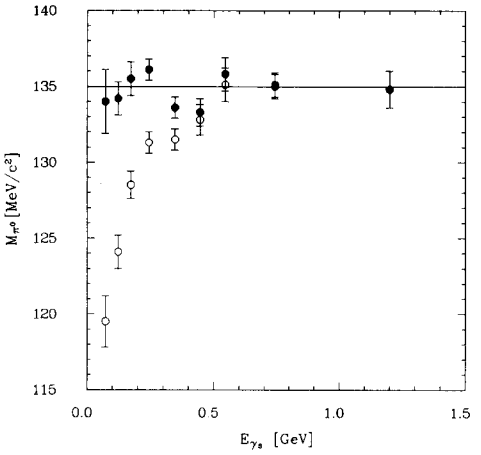

Fig. 1. π^0 mass reconstructed from γ_c and γ_s (see text) as a function of the energy of γ_s before (open circles) and after correction (full dots). The line indicates the table value of the π^0 mass

of E_{γ_s}. The difference between the table value and the reconstructed π^0 mass in Fig. 1 allows the derivation of the correction function.

2.3 π^0 meson analysis

In the sample of multihadron events obtained by the procedure described in [4], photons were selected which fulfilled two conditions: a minimum energy exceeding $E_\gamma \geqq 100$ MeV was required and the quantity f_{LAT}, characterizing the transverse energy deposition of the electromagnetic shower in the calorimeter [14], had to be smaller than a specific value chosen such that 95% of all nonoverlapping photon clusters were accepted. A simulation showed that more than 60% of all π^0 mesons reconstructed from overlapping photons were rejected by this cut.

The measured π^0 mass distributions for different intervals of the scaled energy

$$z = \frac{2E_{\pi^0}}{\sqrt{s}}$$

are shown in Fig. 2a–d. The background below the π^0 meson signal was derived from simulated events where only those photons which were produced in the decay of two different π^0 mesons were combined. This simulated background was normalized to the data in the mass interval $0.25\,\mathrm{GeV/c^2} \leqq m_{\gamma\gamma} \leqq 0.5\,\mathrm{GeV/c^2}$. Since the shape of the background depends on the topology and the photon spectra in the event sample, an appropriate mixture of simulated continuum events and direct Υ decays was used to estimate the background shape for the data sample collected at the energy of the Υ resonances.

The π^0 signals after background subtraction have been compared to invariant mass distributions of γ

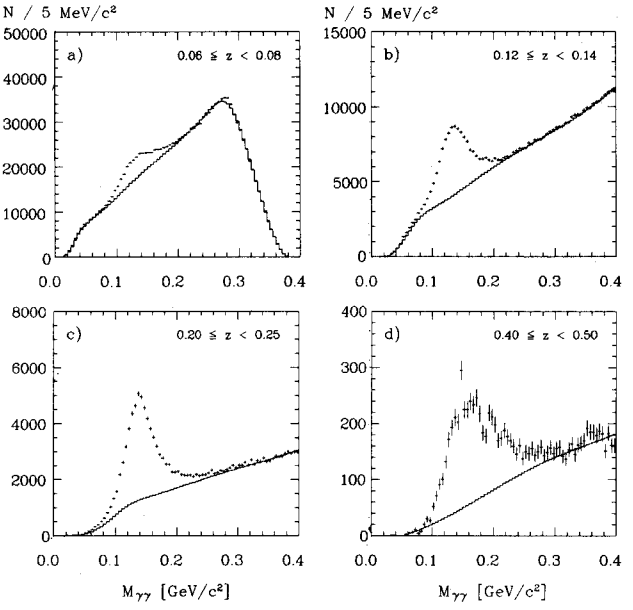

Fig. 2a–d. Two photon invariant mass distributions in different z bins ($\Upsilon(1S)$ data). The full lines represent the background distributions derived from Monte Carlo simulations

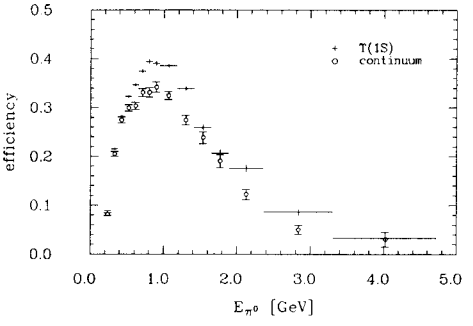

Fig. 3. π^0 reconstruction efficiency for continuum events and direct $\Upsilon(1S)$ decays

pairs from π^0 meson decays derived from a detailed Monte Carlo simulation [15]. The width of the π^0 signals increases for higher energies (Fig. 2), which is due to the energy and angular resolution of the calorimeter. These effects are properly described by the Monte Carlo simulation.

This event simulation was also used to calculate the acceptance losses due to event selection cuts, geometrical acceptance of the detector, overlap of photon showers with charged and neutral particles and the cuts applied to select photons. Simulated distributions of global event features like charged and neutral multiplicity, event shape and transverse shape of electromagnetic showers were carefully compared to measured data and have been found to be in good agreement. In Fig. 3 the total efficiency for continuum events and direct $\Upsilon(1S)$ decays is plotted as a function

of the π^0 meson energy. The increase of the acceptance at low energies can be traced to the cut applied on the photon energy, while the decrease of acceptance at high energies is due to smaller opening angles between the photons from π^0 decays at high energies, which leads to an enhancement of the overlap probability. The π^0 reconstruction efficiency for continuum events is smaller than that for direct Υ decays because the latter are more isotropic thus reducing the losses due to overlaps with other charged or neutral tracks.

The continuum spectra were derived by adding the acceptance corrected rates obtained at various CMS energies which were scaled in an appropriate way using the measured luminosity and the $1/s$ dependence of the cross sections. Radiative corrections were applied using the Lund Monte Carlo program [16]. The contribution of vector meson resonances with a mass below the centre-of-mass energies of DORIS was taken into account as discussed in detail in [12]. The differential cross section for π^0 production from direct decays of the Υ meson was derived from the measured cross section at this energy by subtracting the measured continuum cross section scaled by the CMS energy and corrected for the vacuum polarization contribution [4].

Possible sources of systematic errors were carefully studied. The main contributions are due to event selection (2%), luminosity measurement (5%), differences between Monte Carlo simulation and data (5%), background subtraction (4%) and photon energy smearing (3%). The values given in brackets are typical values, although for $z > 0.5$ the systematic uncertainties are larger. Adding these contributions in quadrature, the total systematic error is 9%.

2.4 η meson analysis

The study of η production was quite similar to the π^0 analysis. For the η, a photon cut of $E_\gamma \geqq 50$ MeV was applied. In the η mass region a reduction of the background due to photons from π^0 meson decays was necessary. This was achieved by rejecting all photons which, when combined with another photon of the event, gave an invariant mass compatible with the π^0 meson mass. The variable used is

$$\chi^2_{\pi^0} = \frac{(m_{\gamma\gamma} - m_{\pi^0})^2}{(\Delta m_{\gamma\gamma})^2}$$

where $\Delta m_{\gamma\gamma}$ is the uncertainty of the $\gamma\gamma$ invariant mass $m_{\gamma\gamma}$. All photons with $\chi^2_{\pi^0} \leqq 4$ were not considered further in the analysis.

The resulting invariant mass spectra are shown in Fig. 4a–d for different z intervals. For $z \leqq 0.30$ no reliable signal could be extracted. A description of

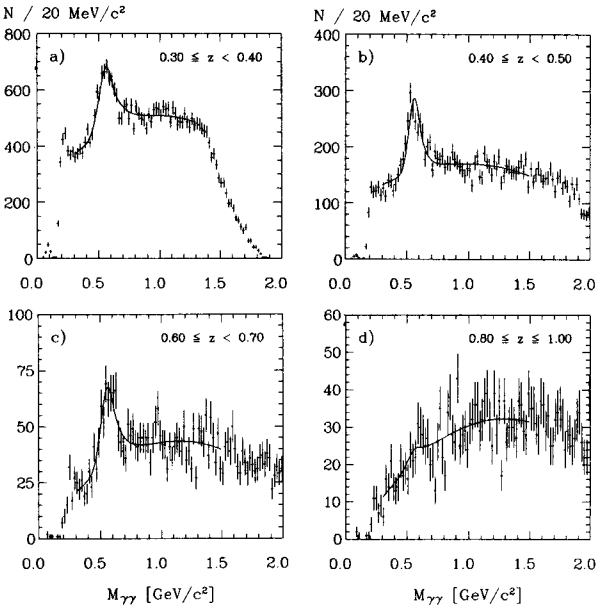

Fig. 4a–d. Two photon invariant mass distributions in different z bins after π^0 suppression ($\Upsilon(1S)$ data). The full lines show the results of a fit as described in the text

the background in the η mass region analogous to that used for π^0 mesons gave poor results. On the other hand the η signal is far away from threshold, so that a parametrization of the background using a polynomial is more reliable than for the π^0 signal. Thus a third order polynomial plus a gaussian, with a width derived from Monte Carlo simulations, was chosen to fit the invariant mass spectra. The rates were corrected for the non-gaussian tails of the η signal.

The acceptance was again determined from a detailed Monte Carlo simulation of the detector. The procedure to reduce the background from π^0 decays strongly influences the η reconstruction efficiency. Therefore it has been carefully checked that the spectrum of photons originating from neutral pion decays is sufficiently well reproduced by the Monte Carlo. Faked low energy photons due to noise in the shower counter electronics which are present in the data but not in the simulation also affect the acceptance. To account for efficiency uncertainties caused by inappropriate simulation of the γ spectrum a contribution of 15% to the systematic error has been calculated.

The energy dependence of the acceptance is shown in Fig. 5 for continuum events and for direct Υ decays. The observed shape of the distribution is mainly due to the cut applied to reject the π^0 background. The η spectra were derived from the acceptance corrected rates, including radiative corrections for the continuum data. The spectra for direct Υ decays follow from

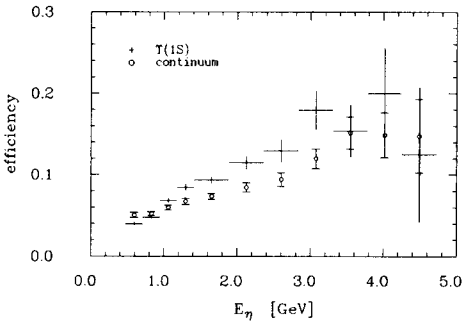

Fig. 5. η reconstruction efficiency for continuum events and direct $\Upsilon(1S)$ decays

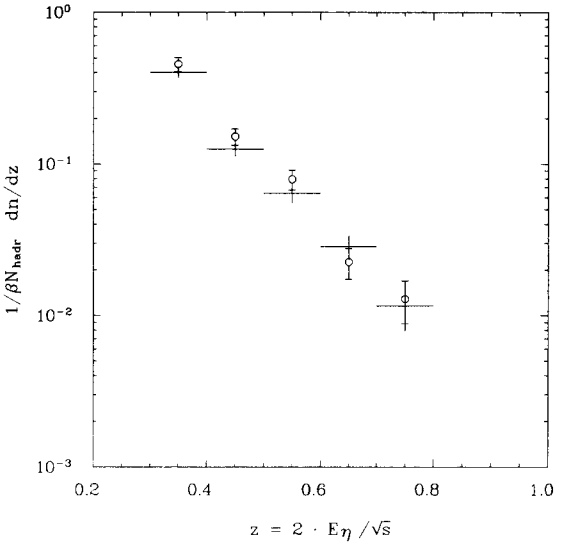

Fig. 6. Inclusive η spectra derived with two different sets of cuts ($\Upsilon(1S)$ data, no continuum subtraction). Crosses: $E_\gamma > 50$ MeV, π^0 suppression; open circles: $E_\gamma > 200$ MeV, no additional π^0 suppression

the measured rates by subtracting the contribution from continuum events and vacuum polarization.

To study systematic uncertainties an alternative method was used to extract the η signal, similar to that employed in the π^0 study. Only photons with an energy $E_\gamma > 200$ MeV were taken into account to calculate the $\gamma\gamma$ invariant mass. No further attempt to suppress the contribution from π^0 decays was made. Again a clear η peak is observed, although the background is higher than in the previous analysis. The remaining steps of the analysis proceed as described above. The two results are in good agreement as demonstrated by Fig. 6 for η production in $\Upsilon(1S)$ decays.

The overall systematic error is calculated to be 18%, where the main difference from the π^0 study is the larger uncertainty in the acceptance determination and in the background estimation.

3 Results

3.1 Inclusive π^0 meson spectra

The measured π^0 spectra are shown in Fig. 7a–c and Tables 5–6 for the continuum and for direct decays of the $\Upsilon(1S)$ and $\Upsilon(2S)$ meson. The corrections discussed in Sect. 2.3 have been applied. The full lines represent fits of the function

$$\frac{1}{\beta N_{\text{hadr}}} \frac{dn_{\pi^0}}{dz} = A_1 e^{-b_1 z} + A_2 e^{-b_2 z} \tag{1}$$

to the data. The respective fit parameters are presented in Table 1. The inclusive π^0 spectrum for direct $\Upsilon(1S)$ and $\Upsilon(2S)$ decays decreases faster with increasing z than the π^0 spectrum in the continuum. This difference is attributed to the different parton configuration of the basic process, namely $q\bar{q}$-pairs for the continuum and three gluons in direct Υ decays.

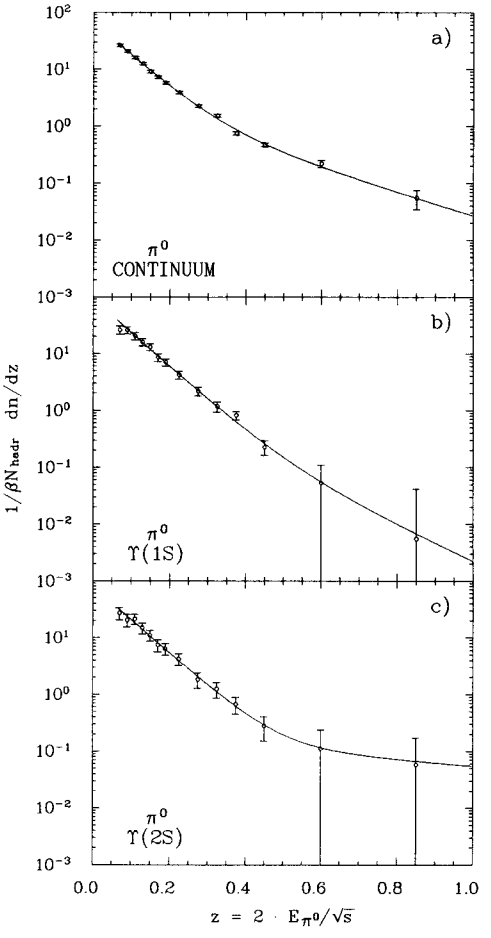

Fig. 7a–c. Inclusive π^0 spectra from continuum events and direct $\Upsilon(1S)$ and $\Upsilon(2S)$ decays. The solid lines represent fits to the data as described in the text

In Fig. 8 and Fig. 9, the continuum data from this experiment are compared with data collected at other energies [9, 10, 17]. All measurements agree nicely with each other. Note also the good agreement between the ARGUS and CLEO data [2] for direct $\Upsilon(1S)$ decays shown in Fig. 10. In Fig. 11a, b the measured π^0 spectra are compared to model predictions

Table 1. Parameters of a fit to the inclusive π^0 spectra

	A_1	b_1	A_2	b_2
Continuum				
$\sqrt{s}=9.46$ GeV	65.6 ± 2.5	14.1 ± 0.6	3.2 ± 1.2	4.8 ± 0.7
$\Upsilon(1S)$	92.1 ± 4.4	14.2 ± 1.0	2.6 ± 7.0	7.1 ± 3.4
$\Upsilon(2S)$	80.7 ± 6.1	13.6 ± 0.6	0.2 ± 0.4	1.3 ± 2.7

Table 2. Mean π^0 multiplicities

	Data	LUND	Webber
Continuum			
$\sqrt{s}=9.46$ GeV	$3.22\pm0.07\pm0.31$	3.58	3.62
$\Upsilon(1S)$	$3.97\pm0.23\pm0.38$	4.25	4.10
$\Upsilon(2S)$	$3.67\pm0.14\pm0.35$		

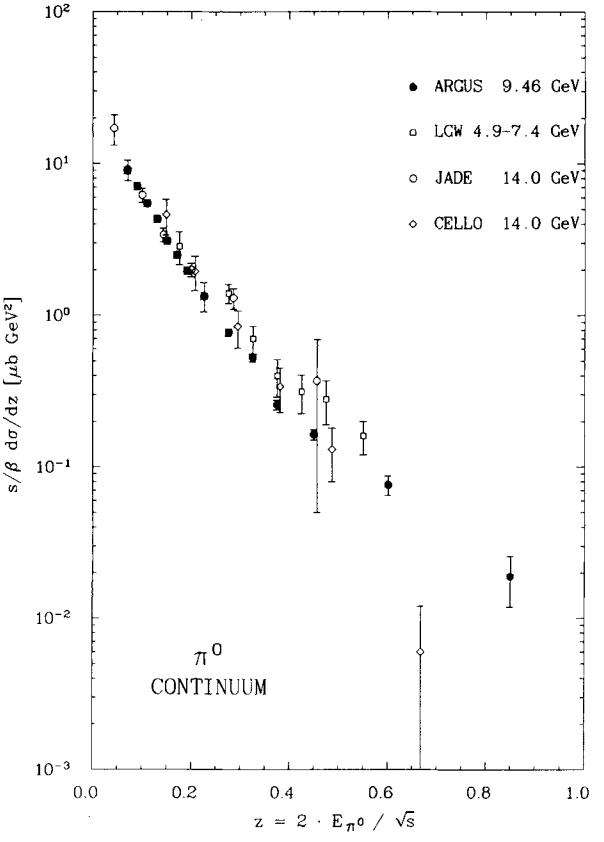

Fig. 8. Comparison of differential π^0 continuum cross section with results of other experiments at similar CMS energies (statistical and systematic errors added in quadrature)

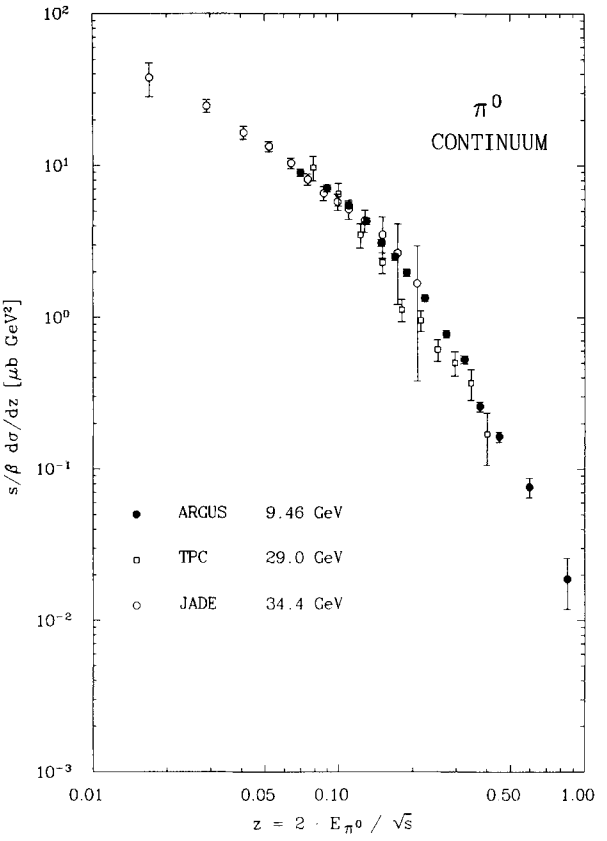

Fig. 9. Comparison of differential π^0 continuum cross section with results of other experiments at higher CMS energies (statistical and systematic errors added in quadrature)

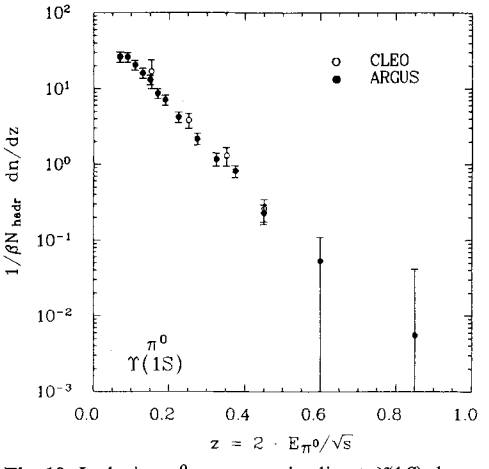

Fig. 10. Inclusive π^0 spectrum in direct $\Upsilon(1S)$ decays compared to a CLEO result

[16, 18]. Good agreement is observed for $z<0.5$, while large differences can be seen for $z>0.5$, particularly for the Webber shower Monte Carlo [18]. This trend was already noted by other experiments [19].

Finally one can integrate the inclusive spectrum to determine the mean number of π^0 mesons pro-

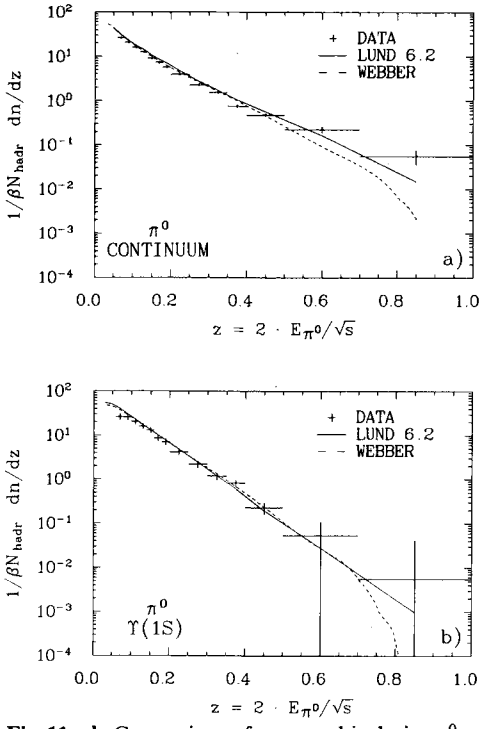

Fig. 11a, b. Comparison of measured inclusive π^0 spectrum in continuum events and direct $\Upsilon(1S)$ decays to Monte Carlo predictions

Table 3. Parameters of a fit to the inclusive η spectra

	A	b
Continuum		
$\sqrt{s}=9.46$ GeV	4.2 ± 1.1	7.38 ± 0.38
$\Upsilon(1S)$	27.4 ± 11.0	11.86 ± 0.67
$\Upsilon(2S)$	11.3 ± 6.1	9.29 ± 0.65

Table 4. Mean η multiplicities

	ARGUS	LUND	Webber
Continuum			
$\sqrt{s}=9.46$ GeV	$0.19\pm0.04\pm0.04$	0.43	0.55
$\Upsilon(1S)$	$0.40\pm0.14\pm0.09$	0.57	0.49
$\Upsilon(2S)$	$0.32\pm0.14\pm0.07$		

CELLO	JADE	HRS	MARK II
$\sqrt{s}=35$ GeV	$\sqrt{s}=34$ GeV	$\sqrt{s}=29$ GeV	$\sqrt{s}=29$ GeV
0.63 ± 0.12	0.64 ± 0.15	0.58 ± 0.10	$0.62\pm0.17\pm0.15$

duced per event

$$\langle n_{\pi^0}\rangle = \frac{1}{N_{\text{hadr}}}\int_{z_0}^{1}\frac{dn_{\pi^0}}{dz}dz$$

$$z_0 = \frac{2m_{\pi^0}}{\sqrt{s}}. \qquad (2)$$

Table 5. Inclusive π^0 spectrum in the continuum

z	$\frac{1}{\beta N_{\text{hadr}}}\frac{dn_{\pi^0}}{dz}$	$\frac{s}{\beta}\frac{d\sigma}{dz}$ (μb GeV^2)
0.06–0.08	$26.3\ \pm0.7\ \pm2.4$	$9.00\ \pm0.24\ \pm0.81$
0.08–0.10	$20.7\ \pm0.5\ \pm1.9$	$7.08\ \pm0.16\ \pm0.64$
0.10–0.12	$16.0\ \pm0.4\ \pm1.4$	$5.47\ \pm0.12\ \pm0.49$
0.12–0.14	$12.6\ \pm0.3\ \pm1.2$	$4.31\ \pm0.09\ \pm0.40$
0.14–0.16	$9.06\ \pm0.20\ \pm0.83$	$3.10\ \pm0.07\ \pm0.28$
0.16–0.18	$7.31\ \pm0.17\ \pm0.72$	$2.50\ \pm0.06\ \pm0.23$
0.18–0.20	$5.75\ \pm0.14\ \pm0.54$	$1.97\ \pm0.05\ \pm0.18$
0.20–0.25	$3.90\ \pm0.08\ \pm0.37$	$1.33\ \pm0.02\ \pm0.13$
0.25–0.30	$2.26\ \pm0.06\ \pm0.22$	$0.772\pm0.020\pm0.074$
0.30–0.35	$1.54\ \pm0.06\ \pm0.15$	$0.526\pm0.019\pm0.051$
0.35–0.40	$0.754\pm0.041\pm0.072$	$0.258\pm0.014\pm0.025$
0.40–0.50	$0.477\pm0.029\pm0.046$	$0.163\pm0.010\pm0.016$
0.50–0.70	$0.222\pm0.022\pm0.048$	$0.076\pm0.008\pm0.016$
0.70–1.00	$0.055\pm0.015\pm0.026$	$0.019\pm0.005\pm0.009$

Table 6. Inclusive π^0 spectra from direct $\Upsilon(1S)$ and $\Upsilon(2S)$ decays

z	$\frac{1}{\beta N_{\text{hadr}}}\frac{dn_{\pi^0}}{dz}(\Upsilon(1S))$	$\frac{1}{\beta N_{\text{hadr}}}\frac{dn_{\pi^0}}{dz}(\Upsilon(2S))$
0.06–0.08	$26.2\ \pm1.1\ \pm2.4$	$27.1\ \pm2.1\ \pm2.4$
0.08–0.10	$26.0\ \pm0.7\ \pm2.3$	$20.5\ \pm1.3\ \pm1.8$
0.10–0.12	$20.4\ \pm0.5\ \pm1.8$	$21.3\ \pm1.1\ \pm1.9$
0.12–0.14	$16.0\ \pm0.4\ \pm1.5$	$14.9\ \pm0.8\ \pm1.4$
0.14–0.16	$13.1\ \pm0.3\ \pm1.2$	$11.0\ \pm0.6\ \pm1.0$
0.16–0.18	$8.62\ \pm0.25\ \pm0.79$	$7.40\ \pm0.47\ \pm0.68$
0.18–0.20	$7.03\ \pm0.21\ \pm0.66$	$6.31\ \pm0.40\ \pm0.59$
0.20–0.25	$4.18\ \pm0.11\ \pm0.39$	$4.19\ \pm0.22\ \pm0.39$
0.25–0.30	$2.17\ \pm0.08\ \pm0.21$	$1.82\ \pm0.16\ \pm0.17$
0.30–0.35	$1.17\ \pm0.07\ \pm0.11$	$1.23\ \pm0.15\ \pm0.12$
0.35–0.40	$0.818\pm0.060\pm0.079$	$0.66\ \pm0.11\ \pm0.06$
0.40–0.50	$0.227\pm0.033\pm0.022$	$0.275\pm0.075\pm0.026$
0.50–0.70	$0.053\pm0.025\pm0.012$	$0.111\pm0.061\pm0.024$
0.70–1.00	$0.006\pm0.022\pm0.003$	$0.058\pm0.078\pm0.027$

Table 7. Inclusive η spectrum in the continuum

z	$\frac{1}{\beta N_{\text{hadr}}}\frac{dn_{\eta}}{dz}$	$\frac{s}{\beta}\frac{d\sigma}{dz}$ (μb GeV^2)
0.30–0.40	$0.364\pm0.061\pm0.068$	$0.1294\pm0.0217\pm0.0243$
0.40–0.50	$0.134\pm0.024\pm0.025$	$0.0478\pm0.0085\pm0.0090$
0.50–0.60	$0.065\pm0.015\pm0.012$	$0.0231\pm0.0055\pm0.0043$
0.60–0.70	$0.054\pm0.011\pm0.010$	$0.0191\pm0.0041\pm0.0036$
0.70–0.80	$0.017\pm0.007\pm0.003$	$0.0062\pm0.0023\pm0.0012$
0.80–1.00	$0.005\pm0.003\pm0.001$	$0.0016\pm0.0010\pm0.0003$

Parametrization (1) has been used to describe the data and to extrapolate to $z=z_0$. The systematic uncertainty in the extrapolation was estimated to be 3% by applying the procedure to a Monte Carlo generated data sample. The results are collected in Table 2 and compared with model predictions, which are in satisfactory agreement.

Table 8. Inclusive η spectrum from direct $\Upsilon(1S)$ decays

z	$\frac{1}{\beta N_{\text{hadr}}}\frac{dn_\eta}{dz}$
0.30–0.40	0.441 ±0.067 ±0.082
0.40–0.50	0.119 ±0.027 ±0.022
0.50–0.60	0.062 ±0.019 ±0.012
0.60–0.70	0.009 ±0.012 ±0.002
0.70–0.80	0.0064±0.0079±0.0012
0.80–1.00	−0.0027±0.0035±0.0005

Table 9. Inclusive η spectrum from direct $\Upsilon(2S)$ decays

z	$\frac{1}{\beta N_{\text{hadr}}}\frac{dn_\eta}{dz}$
0.30–0.40	0.412±0.146±0.077
0.40–0.50	0.170±0.063±0.032
0.50–0.60	0.115±0.043±0.022
0.60–0.70	0.005±0.028±0.001
0.70–0.80	0.027±0.020±0.005
0.80–1.00	−0.011±0.013±0.002

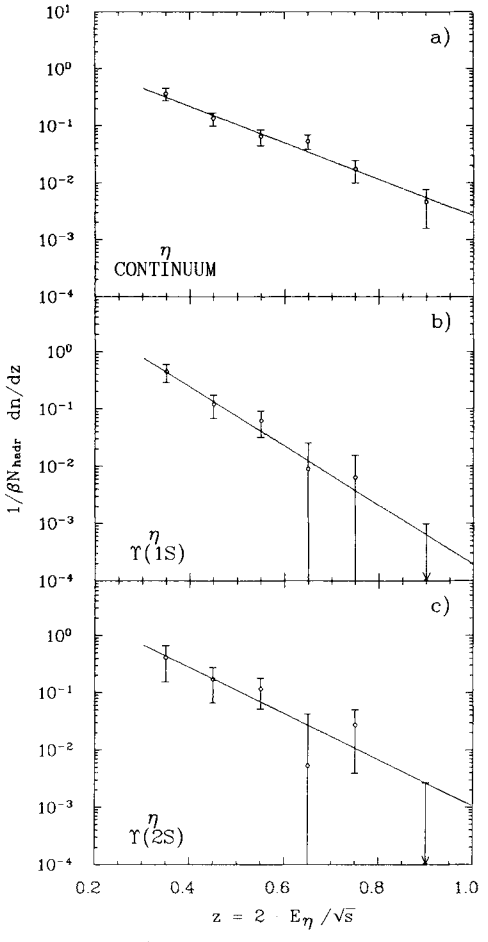

Fig. 12a–c. Inclusive η spectra from continuum events and direct $\Upsilon(1S)$ and $\Upsilon(2S)$ decays. The solid lines represent fits to the data as described in the text

3.2 Inclusive η meson spectra

The measured inclusive spectra of η mesons are shown in Fig. 12a–c and Tables 7–9 for continuum data and direct $\Upsilon(1S)$ and $\Upsilon(2S)$ decays. Data are available for $z>0.30$. To reduce the number of free parameters only a simple exponential

$$\frac{1}{\beta N_{\text{hadr}}}\frac{dn_\eta}{dz}=Ae^{-bz} \tag{3}$$

has been used to fit the spectra. The results are shown in Fig. 12, while the determined values for the parameters are collected in Table 3. Again the η meson spectrum for direct $\Upsilon(1S)$ decays is steeper than the spectrum measured in the continuum.

The measured η spectrum in the continuum is compared to spectra obtained by other experiments at different CMS energies [9, 20–22] in Fig. 13. In Fig. 14a, b the data are compared with model predictions [16, 18]. Within the large uncertainties they agree well with each other.

The mean number of η mesons per event again was derived using (2) and (3). Note however that for

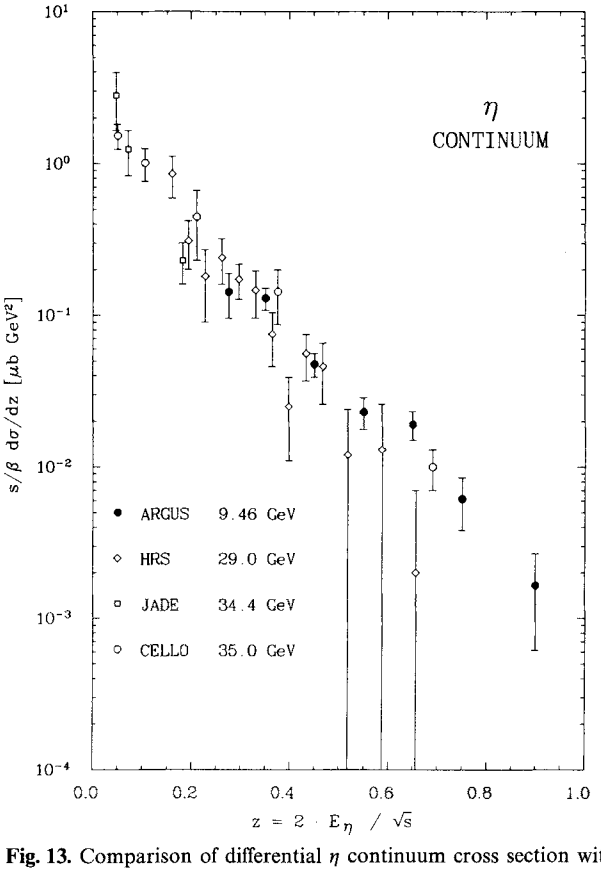

Fig. 13. Comparison of differential η continuum cross section with results of other experiments at higher CMS energies (statistical errors only)

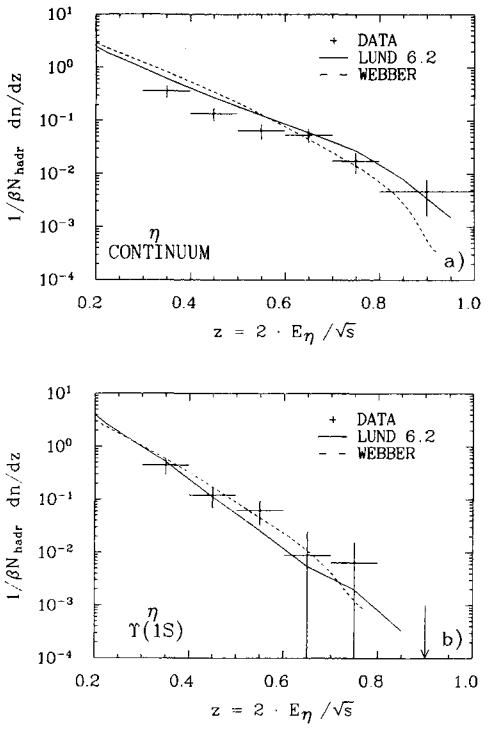

Fig. 14a, b. Comparison of measured inclusive η spectrum in continuum events and direct $\Upsilon(1S)$ decays to Monte Carlo predictions

η mesons the data have to be extrapolated over a substantial range in z. Hence the additional systematic error is larger than for π^0 mesons. By applying the same extrapolation procedure to Monte Carlo generated η spectra the error was estimated to be 15%. The η meson multiplicities are given in Table 4 and compared to results of other experiments [9, 20–22] as well as to model predictions.

The relative production rates of η and π^0 mesons in quark and gluon jets have been of theoretical interest [7]. Peterson and Walsh predicted an enhanced η production in gluon jets in comparison with quark jets, by as much as a factor of 3 to 10. Taking only leading η mesons with $z>0.3$, one finds n_η $(z>0.3)$ $=0.062\pm0.007\pm0.011$ in the continuum and n_η $(z>0.3)=0.060\pm0.007\pm0.011$ in direct $\Upsilon(1S)$ decays. In agreement with the conclusions drawn in [4] from the study of ϕ meson production, we find no enhancement of the production of isosinglet mesons in gluon jets in comparison with quark jets.

Comparing production rates in the continuum and in direct $\Upsilon(1S)$ decays one obtains a ratio of multiplicities of 1.23 ± 0.17 for π^0 mesons and of 2.1 ± 1.2 for η mesons, respectively. The π^0 result is in excellent agreement with the $\pi^\pm$ result derived by the ARGUS experiment [3]. No definite conclusion can be drawn concerning the η ratio because of the large error.

4 Summary

Using the ARGUS detector, we have measured the π^0 and η meson spectra in the continuum and for direct $\Upsilon(1S)$ and $\Upsilon(2S)$ decays. The π^0 data agree with results of other experiments. The π^0 meson multiplicity is determined to be $3.22\pm0.07\pm0.31$ in the continuum and $3.97\pm0.23\pm0.38$ in direct $\Upsilon(1S)$ decays. These results are in good agreement with the corresponding average values of $\langle n_{\pi^\pm}\rangle/2=3.19\pm0.06$ (continuum) and $\langle n_{\pi^\pm}\rangle/2=3.78\pm0.07$ ($\Upsilon(1S)$ decays) for charged pions [3]. The production rates for η mesons are $0.19\pm0.04\pm0.04$ (continuum) and 0.40 ± 0.14 ±0.09 ($\Upsilon(1S)$ decays). The predicted enhancement of high momentum η meson production in gluon fragmentation in comparison with quark jets [7] is not substantiated by the data.

Acknowledgements. It is a pleasure to thank U. Djuanda, E. Konrad, E. Michel, and W. Reinsch for their competent technical help in running the experiment and processing the data. We thank Dr. H. Nesemann, B. Sarau, and the DORIS group for the excellent operation of the storage ring. The visiting groups wish to thank the DESY directorate for the support and kind hospitality extended to them.

References

1. H. Albrecht et al., DASP II: Phys. Lett. 102B (1981) 291
2. S. Behrends et al., CLEO: Phys. Rev. D31 (1985) 2161
3. H. Albrecht et al., ARGUS: Z. Phys. C – Particles and Fields 44 (1989) 547
4. H. Albrecht et al., ARGUS: Z. Phys. C – Particles and Fields 41 (1989) 557
5. H. Albrecht et al., ARGUS: Z. Phys. C – Particles and Fields 39 (1988) 177
6. H. Albrecht et al., ARGUS: Phys. Lett. 215B (1988) 429
7. I. Montvay, Phys. Lett. 84B (1979) 331; C. Peterson, T.F. Walsh: Phys. Lett. 91B (1980) 455
8. W. Bartel et al., JADE: Phys. Lett. 130B (1983) 454
9. H.J. Behrend et al., CELLO: Z. Phys. C – Particles and Fields 20 (1983) 207; W. Bartel et al., JADE: Z. Phys. C – Particles and Fields 28 (1985) 343; W. Braunschweig et al., TASSO: Z. Phys. C – Particles and Fields 33 (1986) 13
10. H. Aihara et al., TPC: Z. Phys. C – Particles and Fields 27 (1985) 187
11. H. Albrecht et al., ARGUS: Nucl. Instrum. Methods. A275 (1989) 1
12. A. Drescher: thesis, Universität Dortmund 1987
13. A. Drescher et al.: Nucl. Instrum. Methods A249 (1986) 277
14. A. Drescher et al.: Nucl. Instrum. Methods A237 (1985) 464
15. H. Gennow: SIMARG – A Program to simulate the ARGUS Detector, DESY F15-85-02 (1985)
16. B. Andersson et al.: Phys. Rep. 97 (1983) 33
17. D.L. Scharre et al., LGW: Phys. Rev. Lett. 41 (1978) 1005
18. G. Marchesini, B.R. Webber: Nucl. Phys. B238 (1984) 1; B.R. Webber: Nucl. Phys. B238 (1984) 492
19. M. Derrick et al., HRS: Phys. Lett. 164B (1985) 199
20. G. Wormser et al., MARK II: Phys. Rev. Lett. 61 (1988) 1057
21. S. Abachi et al., HRS: Phys. Lett. B205 (1988) 111
22. H.J. Behrend et al., CELLO: DESY 89-008